EUROPEAN FUSION DEVELOPMENT AGREEMENT

EFDA–JET–CP(04)03-34

J.S. Lönnroth, W. Fundamenski, G. Corrigan, V. Parail, J. Spence
and JET EFDA Contributors

Modelling of ELM Heat Pulse Propagation with the Integrated Core-Edge Transport Code COCONUT

Modelling of ELM Heat Pulse Propagation with the Integrated Core-Edge Transport Code COCONUT

J.S. Lönnroth[1], W. Fundamenski[2], G. Corrigan[2], V. Parail[2], J. Spence[2]
and JET EFDA Contributors*

[1]Association EURATOM-Tekes, Helsinki University of Technology, Finland
[2]EURATOM/UKAEA Fusion Association, Culham Science Centre, Abingdon, Oxon, OX14 3DB, UK
** See annex of J. Pamela et al, "Overview of Recent JET Results and Future Perspectives", Fusion Energy 2002 (Proc. 19th IAEA Fusion Energy Conference, Lyon (2002).*

Preprint of Paper to be submitted for publication in Proceedings of the
31st EPS Conference,
(London, UK. 28th June - 2nd July 2004)

Transport in the Scrape-Off Layer (SOL), especially during transient events, such as Edge Localized Modes (ELMs), is not fully understood. Normally longitudinal transport along the magnetic field lines dominates over perpendicular transport across the field lines, leading to large ELM-driven heat and particle fluxes at the divertor plates. The parallel motion along the field lines is limited to the convective speed of the particles. As a consequence of this, each ELM gives rise to two distinct responses at the targets, first an electron heat pulse a few microseconds after the start of the ELM and then of the order of 100 ms later by an ion heat pulse. The ELMs are generally localized at the outer midplane of the torus-shaped plasma. Therefore, the propagation time to the inner target is longer than that to the outer target, typically 300 ms versus 100 ms for the ion heat pulse at JET [1].

In this paper, the propagation towards the targets of a heat pulse induced at the outer midplane is studied with the integrated transport code COCONUT, which is a self-consistent coupling between the 1.5D core transport code JETTO [2] and the 2D edge transport code EDGE2D / NIMBUS [3]. In a typical COCONUT simulation, the boundary between the 1D and 2D grids is at the separatrix. JETTO calculates the heat fluxes and transport coefficients in the core and passes their values at the separatrix as boundary conditions for EDGE2D, whereas EDGE2D calculates the corresponding quantities in the SOL and passes their separatrix values as boundary conditions for JETTO [4]. Both codes are called at each time step.

In the simulations described in this paper, the Edge Transport Barrier (ETB) is represented by a suppression of all perpendicular transport coefficients to a uniform ion neo-classical level in a narrow region just inside the separatrix on the one-dimensional grid. Inter-ELM perpendicular transport in the SOL, where the grid is two-dimensional, is kept constant at the same level as in the ETB.

Longitudinal transport in the SOL is calculated according to the 21 moment approximation. It can be scaled by adjusting the coefficients as in the so-called flux limiter, defined as

$$\chi_{\parallel} = \frac{\chi_{\parallel 0 s}}{1 + \left| \frac{n_s \chi_{\parallel 0 s} \nabla T_s}{\alpha_s \nabla n_s c_s T_s} \right|} \qquad (1)$$

Here, the subscript s refers to either ions or electrons. In the simulations in this paper, the transmission factors default to $\alpha_i = \alpha_e = 0.2$.

An ELM-driven heat pulse is induced in the following way: In the ETB just inside the separatrix at the edge of the JETTO grid, the perpendicular transport coefficients are enhanced radially uniformly by a factor of 100 from the inter-ELM ion neo-classical level.

The enhancement is applied for 100μs and is preceded as well as followed by short ramp-up and ramp-down times, respectively, of 1μs. This generates a powerful outflux of heat from the core to the SOL. In the SOL, where the grid is two-dimensional, the perpendicular transport coefficients are enhanced poloidally non-uniformly during the ELM. More specifically, the poloidal enhancement profile is a Gaussian distribution centred at the outer midplane in order to take into account the fact

that ELMs generally occur at the outer midplane. The half width of the distribution is $\pi/16$ in terms of poloidal angle and its amplitude is chosen in such a way that the poloidal average matches the enhancement amplitude in the ETB, where the grid is one-dimensional. Figure 1(a), which shows ion thermal conductivity as a function of the poloidal distance just outside the separatrix during an ELM, illustrates the poloidal transport enhancement profile used in the simulations.

Radially, perpendicular transport in the SOL is enhanced in different ways. This is illustrated in Fig.1(b), which shows the radial profiles of the perpendicular transport coefficients during an ELM in two different scenarios. First, a radially constant enhancement profile has been used and later a step-function shaped radial profile. In the latter case, perpendicular transport in the inner half of the SOL is again enhanced so that the poloidal average matches the enhancement in the ETB, but in outer half of the ETB the enhancement is only one thousandth of that. A step-shaped radial enhancement profile like the one used here is of course artificial, but yields very similar results to those obtained with a more realistic exponential profile.

The propagation of the ion and electron heat pulses towards the outer and inner targets has been studied. Figure 2 shows the ion and electron heat fluxes as a function of time measured at the wall, the outer target and the inner target in the scenario with a radially constant enhancement of radial transport. Contrary to what is seen in most experiments, both the ion and electron heat fluxes to the wall are enormous, about 600MW and 200MW, respectively at peak. For comparison, the electron heat fluxes at the outer and inner targets peak at 175MW and 95MW, respectively. The ion heat fluxes at the targets are negligible, of the order of 10MW at peak, as most of the power in the ion channels goes to the wall. Clearly, the heat transport in the radial direction is too effective especially in the case of the ions with the radially constant enhancement profile. The heat pulse simply reaches the wall before getting even close to the divertor region.

Figure 3 shows the ion and electron heat fluxes to the wall, outer target and inner target as a function of time in the case of the step-shaped radial transport enhancement during the ELM. It is obvious that the heat flux to the wall is practically zero thanks to the very low level of transport in the outer part of the SOL. Accordingly, the heat fluxes at the targets increase, but not as much as expected. In particular, the ion heat flux is still negligible, at most 15MW at both targets.

It turns out that the heat fluxes measured at the targets are very sensitive to the assumptions of longitudinal transport as well. By increasing the transmission factors from the default $\alpha_i = \alpha_e = 0.2$ by a factor of about five or more, sizeable responses are obtained at both targets. This is illustrated in Fig.4, which shows time traces of the electron and ion heat fluxes and the electron and ion temperatures at the outer and inner targets in the cases $\alpha_i = \alpha_e = 1.0$ and default $\alpha_i = \alpha_e = 3.0$. In each case, the electron heat fluxes are reasonably large. The ion heat fluxes, however, are rather small, in particular with the lower level of longitudinal transport. In fact, the ion temperature at the outer target still does not respond at all with $\alpha_i = \alpha_e = 1.0$. With $\alpha_i = \alpha_e = 3.0$, the response is already significant. In any case, it can be concluded that the electrons carry heat more effectively than the ions. The different propagation times of the ion and electron heat pulses to the outer and

inner targets are also obvious in the plots. The arrival of the electron heat pulse at the outer target looks almost instantaneous with the time resolution used in the figure. The arrival of the electron heat pulse at the inner target occurs a few microseconds later. The propagation of the ion heat pulse is considerably slower, as expected, because the propagation speed is limited by the convective velocity, which is about 60 times smaller for the ions than for the electrons due to the different masses of these particle species. With $\alpha_i = \alpha_e = 1.0$, the propagation times of the ion heat pulse to the outer and inner targets are about 60μs and 160μs, respectively. These times are slightly shorter than the propagation times reported in Ref. [1], which is not surprising, since longitudinal transport has been increased with the flux limiter. With $\alpha_i = \alpha_e = 3.0$, the propagation times are even shorter, as expected.

Overall, this study shows that the heat fluxes at the targets and at the wall depend very sensitively on the assumptions of both perpendicular and longitudinal transport in the SOL during and after the ELM. In particular, too large radial transport in the outer part of the SOL during the ELM leads to an enormous heat flux to the wall. It also seems as if the ions generally carry less heat to the targets than the electrons. Reasonable ion heat pulses are obtained at the targets only by increasing the longitudinal transmission factors suitably. Clearly much more work needs to be done to establish more precisely how the transport model should be fine-tuned in order to reproduce experimental observations.

REFERENCES

[1]. A. Loarte, et al., Plasma Phys. Control. Fusion **44** 1815 (2002).
[2]. G. Cennachi, A. Taroni, JET-IR(88)03 (1988).
[3]. R. Simonini et al., Contrib. Plasma Phys. **34** 368 (1994).
[4]. J.-S. Lönnroth et al. Plasma Phys. Control. Fusion **45** 1689 (2003).

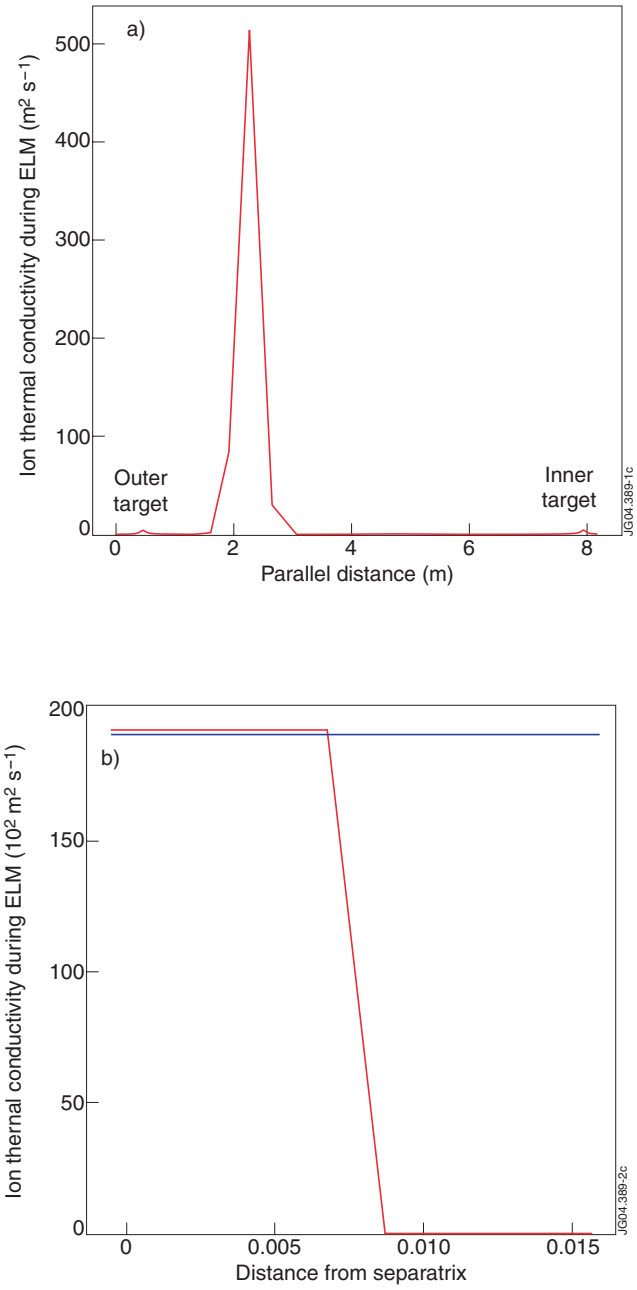

Figure 1. (a) Perpendicular ion thermal conductivity just outside the separatrix during an ELM as a function of the poloidal distance. (b) Perpendicular ion thermal conductivity in the SOL as a function of the radial co-ordinate during an ELM in two different scenarios, one with radially uniform perpendicular transport and onewith radially step-shaped perpendicular transport.

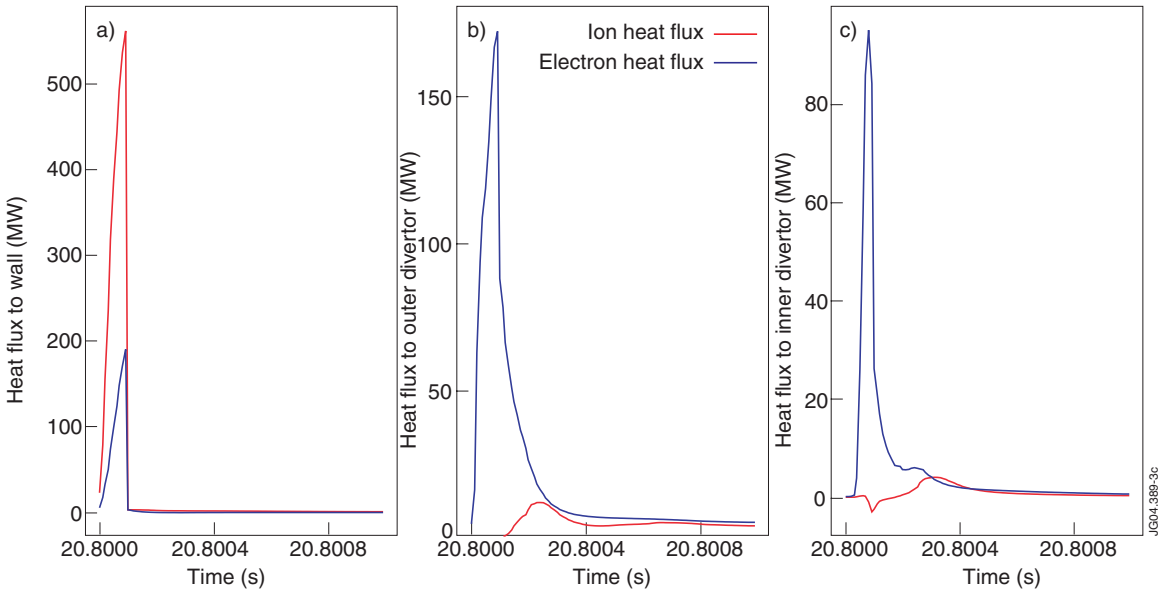

Figure 2. Ion and electron heat fluxes going to (a) the wall, (b) the outer divertor and (c) the inner divertor in the simulation with radially uniform enhancement of perpendicular transport in the SOL.

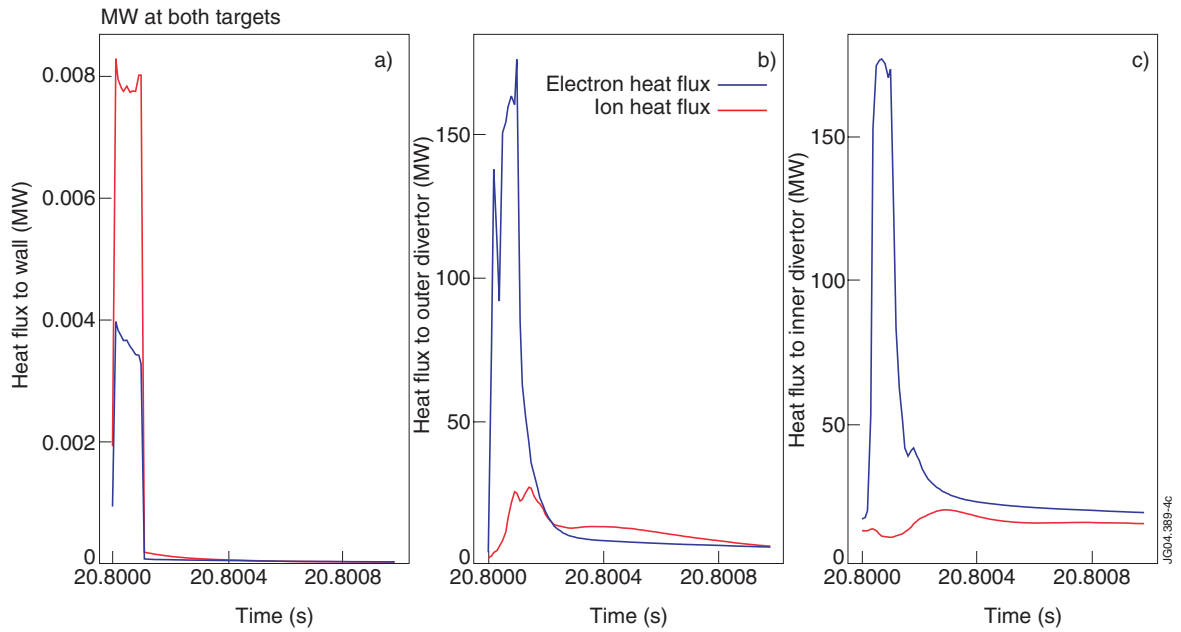

Figure 3. Ion and electron heat fluxes going to (a) the wall, (b) the outer divertor and (c) the inner divertor in the simulation with radially non-uniform enhancement of perpendicular transport in the SOL.

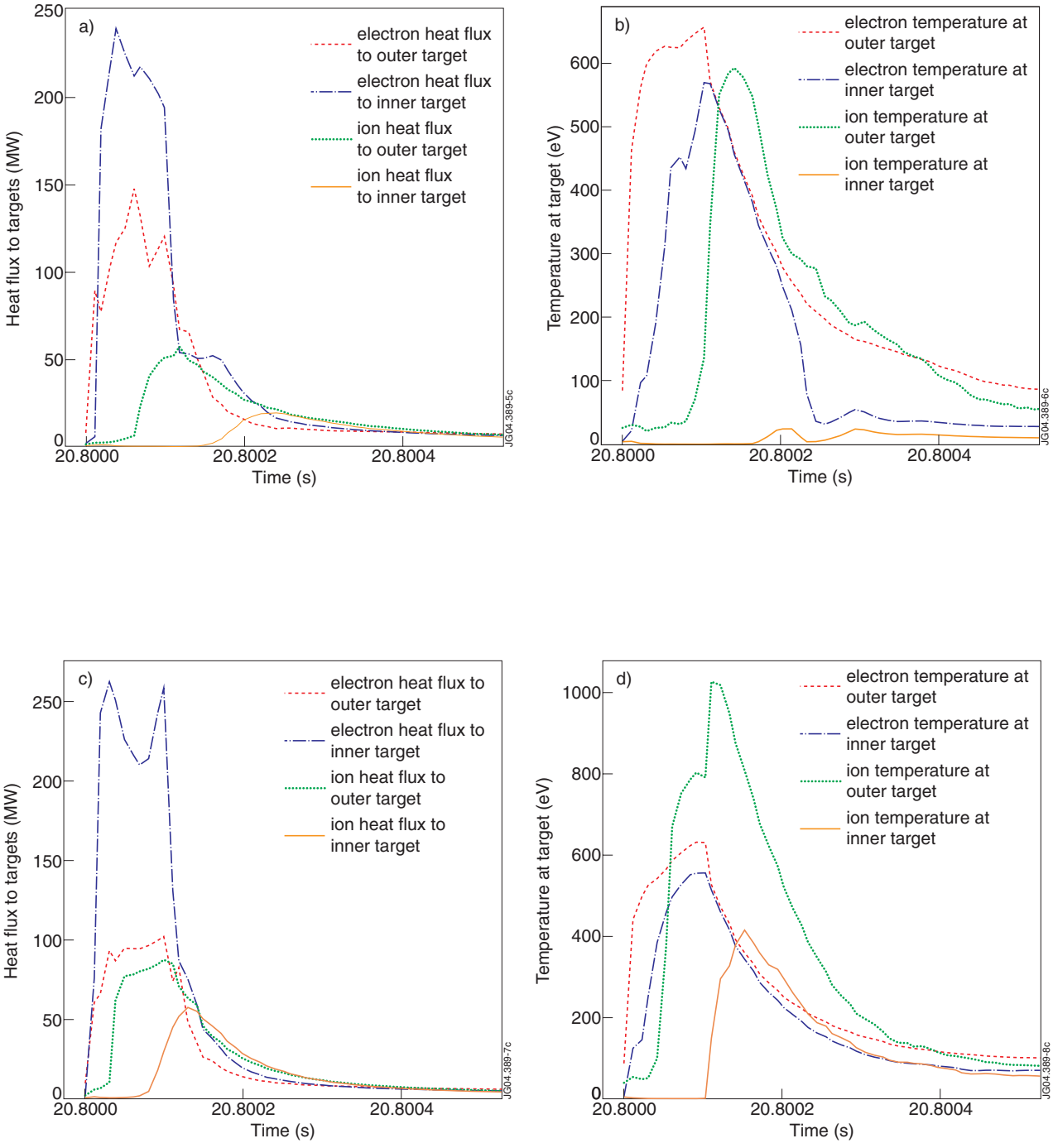

Figure 4. (a) Ion and electron heat fluxes at the outer and inner targets with $\alpha_i = \alpha_e = 1.0$. (b) Ion and electron temperatures at the outer and inner targets with $\alpha_i = \alpha_e = 1.0$. (c) Ion and electron heat fluxes at the outer and inner targets with $\alpha_i = \alpha_e = 3.0$. (d) Ion and electron temperatures at the outer and inner targets with $\alpha_i = \alpha_e = 3.0$.